Journal of Biomolecular NMR, 5 (1995) 397–410
ESCOM

J-Bio NMR 249

Lysine side-chain dynamics derived from ^{13}C-multiplet NMR relaxation studies on di- and tripeptides

Dmitry Mikhailov, Vladimir A. Daragan and Kevin H. Mayo*

Department of Biochemistry, Biomedical Engineering Center, University of Minnesota Health Sciences Center, 420 Delaware Street S.E., Minneapolis, MN 55455, U.S.A.

Received 8 August 1994
Accepted 23 October 1994

Keywords: Peptides; Lysine; Motional dynamics; ^{13}C NMR; Relaxation

Summary

^{13}C NMR relaxation data have been used to determine dipolar auto- and cross-correlation times for the di- and tripeptides GK, KG and GKG, primarily to analyze lysine side-chain motional dynamics. In general, correlation times are largest for backbone positions and decrease on going through the lysine side chain, consistent with the idea of increased mobility at C_δ and C_ε methylenes. Correlation times, however, vary with the peptide ionization state. In the zwitterionic state of GK, for example, both auto- and cross-correlation times are at their maximum values, indicating reduced internal motions probably resulting from intramolecular electrostatic interactions. Modifying the charge state increases motional fluctuations. Activation energies determined from the temperature dependence of CH rotational auto-correlation times at neutral pH are approximately equal for glycine and lysine C_α and lysine C_β and C_γ positions (4.1 ± 0.2 to 4.5 ± 0.2 kcal/mol) and tend to decrease slightly for lysine C_δ and C_ε (3.8 ± 0.2 to 4.3 ± 0.2 kcal/mol). The sign of lysine side-chain cross-correlations could not be explained by using any available rotational model, including one parameterized for multiple internally restricted rotations and anisotropic overall tumbling. Molecular and stochastic dynamics calculations were performed to obtain insight into correlated internal rotations and coupled overall tumbling and internal motions. Relatively strong correlations were found for i,i+1 backbone and lysine side-chain internal bond rotations. Stochastic dynamics calculations were more successful at explaining experimentally observed correlation times. In the fully charged state, a preferred conformation was detected with an all-trans lysine side chain.

Introduction

^{13}C and ^{15}N NMR relaxation allows detailed study of protein backbone and side-chain rotational mobilities. Understanding side-chain motional dynamics is particularly important in the light of their role in protein folding and various binding and enzymatic activities (Dellwo and Wand, 1989; Weaver et al., 1989,1992; Palmer et al., 1991; Nicholson et al., 1992). Rotations of leucine methyl groups, for example, are sensitive to the position of the residue in the protein and to ligand binding (Nicholson et al., 1992). One may expect similar effects in other 'long' hydrophobic and polar/charged side chains. For quantitative modeling of NMR relaxation data of side-chain motions, multiple bond rotations must be considered. This complicates the analysis. Even using a simple model of restricted rotational diffusion (London and Avitable, 1978; Wittebort and Szabo, 1978) to analyze lysine side-chain motions with four internal rotations, various trans/gauche rotomer populations and four internal rotational correlation times and restriction parameters need to be determined. In proteins and large peptides, where spin–lattice T_1 and spin–spin T_2 relaxation times are not equal and $\{^1H\text{-}^{13}C\}$ or $\{^1H\text{-}^{15}N\}$ NOE coefficients are not at their maximum value, multiple experimental parameters can be used in model analyses. Unfortunately, NOE coefficients and auto-correlation functions are not very sensitive to anisotropic motions (Daragan and Mayo, 1992). The situation becomes worse when correlated internal rotations and coupling of internal rotations and overall

*To whom correspondence should be addressed.

Abbreviations: rf, radio frequency; GK, dipeptide glycine-lysine; KG, dipeptide lysine-glycine; GKG, tripeptide glycine-lysine-glycine.

molecular tumbling must be included in the analysis (Moro, 1987; Daragan and Mayo, 1994).

NMR ^{13}C-multiplet relaxation can provide additional motional information. Dipolar cross-correlation spectral densities of different methylene CH bonds are much more reliable and more sensitive to rotational anisotropy than are heteronuclear NOE coefficients. ^{13}C-methylene triplet lines of lysine side chains, for example, demonstrate different relaxation behavior which is related to dipolar and dipolar–CSA (chemical shift anisotropy) cross-correlations (Bain and Lynden-Bell, 1975; Daragan and Mayo, 1993a; Gaisin et al., 1993). Analysis of relaxation data using the dipolar–CSA cross-correlation term is difficult, since the latter is dependent both on peptide geometry and on the orientation of the CSA tensor in the molecular frame. Due to the impossibility to accurately determine the principal values and orientation of the CSA tensor, only dipolar cross-correlations will be considered in the present study.

The goal of this paper is to analyze side-chain motions of lysine residues in tri- and dipeptides (GKG, GK and KG) by using dipolar auto- and cross-correlation times and molecular modeling. Since dipolar cross-correlation times can be accurately measured, these simple peptides provide basic models which can be used to develop better approaches to describe 'long' side-chain dynamics. Previously, we have shown that the ionization states of the N- and C-terminal groups significantly affect auto- and cross-correlation times in short peptides (Daragan and Mayo, 1993b). Similar behavior can be expected in side chains with ionizable groups. This in turn underlies the role of electrostatic interactions in proteins. Before studying backbone and side-chain motional dynamics in a folded protein or in a folding intermediate, it is necessary to establish a working 'baseline' to define internal motional properties present for 'free' rotations in the structurally unconstrained state. Short peptides, not having any long-range interactions, are well suited to achieve this goal.

For dipeptides GK and KG, six auto-correlation times, τ_{CH}, for rotational motions of different methylene and methine ($C_\alpha H$) CH bonds and five cross-correlation times, τ_{HCH} (seven τ_{CH} and six τ_{HCH} for GKG), can be determined. Wittebort and Szabo (1978) and Wittebort et al. (1980) have shown the importance of internal rotational restrictions for lysine side-chain dynamics. In order to fully describe these motional dynamics, one must determine all internal correlation times and restriction parameters (angular limits of internal rotations) for peptide backbone φ and ψ and lysine side-chain χ_1, χ_2, χ_3 and χ_4 bond rotations (see Fig. 1, where the structure of GKG is presented as an example). To describe peptide overall tumbling, six additional parameters are normally needed: three principal values of the rotational diffusion tensor and three angles for orientation of this tensor in the molecular frame. For short peptides, the coupling of overall molecular tumbling and internal rotations must be taken into account (Dong and Richards, 1992; Daragan and Mayo, 1994). This, in turn, gives rise to eight coupling coefficients, one for each internal bond rotation. Additional parameters for correlated internal bond rotations should be considered as well. It becomes readily apparent that any model which attempts to consider all necessary geometric and motional terms will be complicated. The following section outlines some approaches aimed at simplifying the analysis.

Theory

From inversion-recovery NMR experiments, dipolar auto- and cross-correlation times for methylene groups can be determined by using Eq. 1 (Werbelow and Grant, 1977; Grant et al., 1991; Daragan and Mayo, 1993a) which is valid at the extreme narrowing limit:

$$\tau_{CH} = W_C r_{CH}^6 / (Nh^2 \gamma_C^2 \gamma_H^2) \quad (1a)$$

$$\tau_{HCH} = 5(W_o - W_i) r_H^6 / (6h^2 \gamma_C^2 \gamma_H^2) \quad (1b)$$

h is Planck's constant divided by 2π; r_{CH} is the internuclear bond distance between carbon and hydrogen; γ_C and γ_H are the gyromagnetic ratios for carbon and hydrogen nuclei, respectively; W_C is the relaxation rate ($=1/T_1$) of the proton-decoupled ^{13}C resonances; W_o and W_i are initial relaxation rates for outer (average value for left and right) and inner ^{13}C resonances. Equation 1a, where N is the number of bonded hydrogens, can be applied to methine and methyl groups as well. Although Eq. 1a is valid only when the CSA contribution to the relaxation rate is small, Eq. 1b is valid even for large values of CSA. If one takes an average value for left and right ^{13}C-methylene triplet lines, contributions from dipolar–CSA

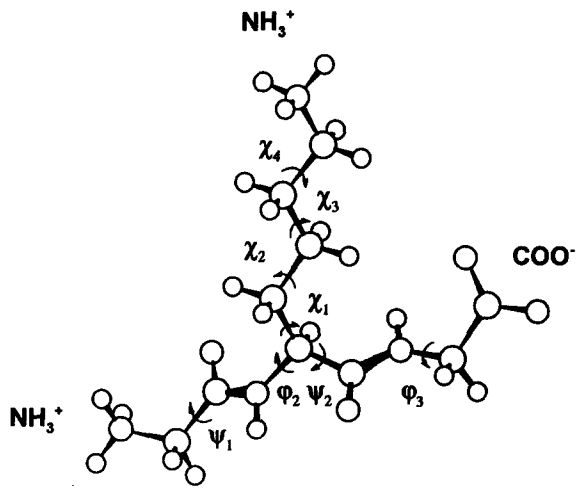

Fig. 1. The molecule GKG, with internal rotations labeled as discussed in the text.

cross-correlations can be excluded. At high magnetic fields, such CSA–dipolar effects can be significant even for short peptides (Daragan and Mayo, 1993a).

The general expression for correlation times can be written as:

$$\tau_{ab} = 4\pi \int_0^\infty \langle Y_{20}(\theta_a^L(t))\, Y_{20}(\theta_b^L(0))\rangle \, dt \qquad (2)$$

where Y_{20} is the second-rank spherical harmonic and $\theta_a^L(t)$ is the angle between some internuclear vector **a** and, for example, the direction of the static magnetic field. The superscript L denotes the laboratory frame. τ_{ab} stands for auto-correlation (**a** = **b**) and cross-correlation (**a** ≠ **b**) times.

Two models used in this paper to analyze ^{13}C NMR relaxation data are outlined below: (1) the model of correlated rotational fluctuations and (2) the model of multiple restricted rotational diffusion with anisotropic overall tumbling.

Model of correlated rotational fluctuations

In this model, we have considered the coupling of overall peptide tumbling and internal rotations by using a 'diffusive' frame (Daragan and Mayo, 1994). Transformation from the laboratory frame to a diffusive frame simplifies calculation of the correlation function in Eq. 2 by allowing it to be factorized as $C_o(t)\, C_{ab}(t)$, where $C_o(t)$ and $C_{ab}(t)$ are the overall and internal correlation times, respectively. Assuming the overall molecular tumbling of the diffusive frame to be isotropic with correlation time τ_o, one can write equations for the correlation time τ_{ab} as:

$$\tau_{ab} = \int_0^\infty \exp(-t/\tau_o)\, C_{ab}^{int}(t)\, dt \qquad (3)$$

where

$$C_{ab}^{int}(t) = 1/2\langle 3(x_a(t)\, x_b(0) + y_a(t)\, y_b(0) + z_a(t)\, z_b(0))^2 - 1\rangle \qquad (4)$$

and $x_a(t)$, $y_a(t)$, $z_a(t)$, $x_b(t)$, $y_b(t)$, $z_b(t)$ are components of the unit vector directed along CH bonds '**a**' and '**b**' in the diffusive frame (Daragan and Mayo, 1994).

Since deviations from isotropic tumbling are not as pronounced for side-chain motions (Levine et al., 1974), only cases of isotropic tumbling for this model have been considered below. $C_{ab}^{int}(t)$ has been calculated by integrating the decay curve from stochastic dynamics calculations. It is important to note that initial values of $C_{ab}^{int}(t)$ are related to molecular geometry by:

$$C_{ab}^{int}(0) = 0.5\,(3\cos^2\theta_{ab} - 1) \qquad (5)$$

where θ_{ab} is the angle between the '**a**' and '**b**' vectors. It should be noted that cross-correlation times can be negative when $\theta_{ab} < 54.7°$ and internal rotations are relatively slow.

In order to describe rotational fluctuations within a potential well, a two-state jump model has been used during computer modeling. This model is capable of describing both molecular dynamics simulations and NMR relaxation data (Daragan and Mayo, 1993b). For this analysis, jumps between $\gamma_o - \gamma$ and $\gamma_o + \gamma$ angles are allowed. γ_o is the equilibrium angle (one each for φ, ψ or χ bond rotations) and γ is the amplitude of the rotational fluctuation. The potential coupling of internal rotations and overall tumbling is treated via use of recoil coefficients, K (Daragan and Mayo, 1994), which describe recoil effects (Moro, 1987) from rotation of one part of a molecule on another part of the molecule. For χ_i rotations, the recoil coefficient may be written as:

$$K_\chi^i = \Delta\chi_i^{end} / (\Delta\chi_i^{end} + \Delta\chi_i^{rest}) \qquad (6)$$

where $\Delta\chi_i^{end}$ and $\Delta\chi_i^{rest}$ are two rotation angles with respect to one of the lysine side-chain bonds about which the rotation is occurring. These angles can be measured in the diffusive or in the laboratory frame (Daragan and Mayo, 1994). The superscripts 'end' and 'rest' refer to the terminal part of the side chain and to the body of the peptide, respectively. $K_\chi^i = 1$ indicates no recoil effects, such that rotation about one of the lysine side-chain C-C methylene bonds does not perturb rotations/tumbling of the rest of the peptide. For φ and ψ bond rotations, K_φ and K_ψ are defined as:

$$K_\varphi = \Delta\varphi_{left} / (\Delta\varphi_{left} + \Delta\varphi_{right}) \qquad (7)$$

$$K_\psi = \Delta\psi_{right} / (\Delta\psi_{right} + \Delta\psi_{left}) \qquad (8)$$

where the subscripts 'left' and 'right' refer to an N- and C-terminal division of the peptide with respect to the C_α-C bond for φ rotation and with respect to the N-C_α bond for ψ rotation. K can vary from 0 to 1, depending on the moments of inertia of the mass on each side of the peptide bond in question and, in general, on intermolecular interactions. For small-amplitude fluctuations, it may be assumed that moments of inertia play the most important role in recoil rotations.

To minimize the number of model parameters, these coupling coefficients have been estimated independently by using the law of conservation of angular momentum. To calculate K_χ coefficients, for example, one can write:

$$K_\chi = 1/(1 + \Delta\chi_{rest}/\Delta\chi_{end}) \approx 1/(1 + I_{end}/I_{rest}) \qquad (9)$$

where I_{end} and I_{rest} are the moments of inertia on both sides of a particular bond. Equation 9 is strictly valid for a symmetrical intramolecular potential $U(\chi) = U(-\chi)$ (Daragan and Mayo, 1994). Results of these calculations, as well as the method of taking into account internal rotational correlations, will be presented below.

Model of multiple restricted rotational diffusion in the presence of anisotropic overall tumbling

To reduce the number of parameters normally required to describe anisotropic overall molecular tumbling, the modified Kirkwood–Steel–Huntress theory (Steel, 1963; Huntress, 1970; Vetrov et al., 1984; Gladkii et al., 1987) has been applied to evaluate the principal values of the rotational diffusion tensor. This approach works better than hydrodynamic theory when a molecule may be represented as a series of linked spheres (Knaus et al., 1980). The theory is based on Steel's equation for diffusion about some axis x with diffusion coefficient D_{xx} (Steel, 1963; Huntress, 1970), written as:

$$D_{xx} = kT\sqrt{\frac{\pi}{2I_{xx}\langle \partial^2 U/\partial\gamma_x^2\rangle}} \tag{10}$$

U is an intermolecular potential; γ_x and I_{xx} are the angle of rotation and the moment of inertia, respectively, about the x-axis; k is the Boltzmann constant, and T is the temperature (K). The angular brackets refer to the ensemble average. The interaction between solute and solvent molecules is assumed to be the sum of (solute atom) – (solvent) pair interactions.

$$U = \sum_k U_{ks} = 4\sum_k \varepsilon_{ks}\left[\left(\frac{\sigma_{ks}}{r_{ks}}\right)^{12} - \left(\frac{\sigma_{ks}}{r_{ks}}\right)^{6}\right] \tag{11}$$

where subscript k refers to one of the solute (peptide) atoms. For simplicity in applying Eq. 10, a Lennard-Jones-type atom–solvent potential was used. The result of the calculation, however, does not depend significantly on the potential used. Under the assumption that (solute atom) – (solvent) pair correlation functions are spherically symmetric and depend only on the distance between the solvent molecule and the nearest solute atom (Vetrov et al., 1984; Gladkii et al., 1987) one can obtain:

$$\begin{aligned}\langle \partial^2 U/\partial\gamma_x^2\rangle &= C(s,T)\sum_k r_{ks}^3 \\ &\times\left[\left(\frac{\partial^2 U_{ks}(r_{ks})}{\partial r_{ks}^2} - \frac{1}{r_{ks}}\frac{\partial U_{ks}(r_{ks})}{\partial r_{ks}}\right)\langle r_y^\circ R_{kz} - r_z^\circ R_{ky}\rangle_{\Omega_{ks}}\right. \\ &\left. + \frac{\partial U_{ks}(r_{ks})}{\partial r_{ks}}\left\langle\frac{R_{ky}^2+R_{kz}^2}{r_{ks}} + r_y^\circ R_{ky} + r_z^\circ R_{kz}\right\rangle_{\Omega_{ks}}\right]\end{aligned} \tag{12}$$

where R_{kx}, R_{ky}, R_{kz} are the coordinates of atom k in the molecular frame and r_x°, r_y°, r_z° are the cosines of the angles between the $\mathbf{r}_{ks}$ vector and the molecular frame axes. Ω_{ks} is the region of polar angles θ_k,φ_k which determines the orientation of the $\mathbf{r}_{ks}$ vector in the molecular frame, where k is the closest solute atom to the 's' solvent molecule. The coefficient C(s,T) depends on the solvent and on the temperature. Although C(s,T) cannot be estimated easily, relative calculations in which this coefficient vanishes have been performed to obtain ratios of the principal values of the rotational diffusion tensor. Gladkii et al. (1987) have shown that $r_{ks} = 1.1\,\sigma_{ks}$ works best for this calculation.

Wittebort and Szabo (1978) have described a model of restricted multiple rotations where overall tumbling has been considered as symmetric top rotational diffusion. Below, we will show by using the modified Kirkwood–Steel–Huntress theory that symmetric top-type anisotropic rotation (with $D_{xx} = D_{yy}$) is a good approximation to describe overall tumbling in the dipeptides KG and GK. In this respect, one can generalize Eq. 3.13 given by Wittebort and Szabo (1978) to obtain an expression for auto- and cross-correlation spectral densities:

$$\begin{aligned}\tau_{ab} = &\sum_{n_1,\ldots,n_j,c_0,c_1,c'_1,\ldots}(6D_{xx} + c_0^2(D_{zz} - D_{xx}) + n_1^2/\tau_1 + \ldots \\ &+ n_j^2/\tau_j)^{-1} \times d^2_{c_0c_1}(\beta_{D1})d^2_{c_0c'_1}(\beta_{D1})\Gamma_{c_1,c'_1,n_1}(\Delta\gamma_1) \\ &\times d^2_{c_1c_2}(\beta_{12})d^2_{c'_1c'_2}(\beta_{12})\Gamma_{c_2,c'_2,n_2}(\Delta\gamma_2)\times\ldots \\ &\times d^2_{c_{j-1}c_j}(\beta_{j-1,j})d^2_{c'_{j-1}c'_j}(\beta_{j-1,j})\Gamma_{c_j,c'_j,n_i}(\Delta\gamma_j)d_{c_j0}(\theta_a)d_{c'_j0}(\theta_b) \\ &\times\cos[(c_1 - c'_1)\alpha_{12} + (c_2 - c'_2)\alpha_{23} + \ldots \\ &+ (c_{j-1} - c'_{j-1})\alpha_{j-1,j} + (c_j\varphi_a - c'_j\varphi_b)]\end{aligned} \tag{13}$$

where

$$\Gamma_{cc'0}(\Delta\gamma) = \frac{\sin(c\Delta\gamma)\sin(c'\Delta\gamma)}{cc'\Delta\gamma^2} \tag{14}$$

and

$$\Gamma_{cc'n}(\Delta\gamma) = \frac{cc'\Delta\gamma^2[\cos(c\Delta\gamma)\cos(c'\Delta\gamma)(1-(-1)^n) + \sin(c\Delta\gamma)\sin(c'\Delta\gamma)(1+(-1)^n)]}{[(c\Delta\gamma)^2 - (n\pi/2)^2][(c'\Delta\gamma)^2 - (n\pi/2)^2]} \tag{15}$$

β_{D1} is the angle between the z-axis of the rotational diffusion tensor and the axis of the first internal rotation. $\beta_{j-1,j}$ is the angle between j–1 and j axes of internal rotation, and $\alpha_{j-1,j}$ is the dihedral angle which specifies the direction about which the restricted rotation occurs. In our case, $\alpha_{i-1,j}$ is the dihedral angle formed by atoms j–2, j–1, j, j+1, where j = 0,1,2,3,4,5 corresponds to C_α, C_β, C_γ, C_δ, C_ε and N atoms of the lysine side chain. $\Delta\gamma_j$ is the amplitude of restricted internal motion for j axes of internal rotation (formed by atoms j–1 and j). $d^2_{c_1c_2}(\beta)$ are elements of the reduced Wigner rotation matrix. τ_i is the correlation time of i-internal rotation (Wittebort and Szabo, 1978) which can be written as:

$$\tau_i = \frac{4\gamma^2}{\pi^2 D_i} \tag{16}$$

where D_i is the diffusion coefficient of the *i*th internal rotation. θ_a, θ_b, φ_a, φ_b are the polar angles of vectors **a** and **b** (C_j-H bonds in our case) in a molecular frame where the z-axis coincides with the C_{j-1}-C_j bond.

Materials and Methods

Peptides

Dipeptides GK and KG were purchased from Sigma Co. and were used without further purification. All samples were dissolved in 0.6 ml D_2O in a 5 mm NMR tube. The peptide concentration was typically 25 mg/ml. The pH was adjusted by adding microliter quantities of NaOD or DCl.

Tripeptide GKG was synthesized on a Milligen Biosearch 9600 automated peptide synthesizer. The procedures used were based on Merrifield solid-phase synthesis utilizing Fmoc-BOP chemistry (Stewart and Young, 1984). After the coupling steps, the peptide support and side-chain protection groups were acid-cleaved (trifluoro acetic acid and scavenger mixture). Crude GKG was analyzed for purity on a Hewlett-Packard 1090M analytical HPLC using a reversed-phase C18 VyDac column. The peptide was about 95% pure. Further purification was done on a preparative reversed-phase HPLC C18 column using an elution gradient of 0–60% acetonitrile with 0.1% trifluoroacetic acid in water. The amino acid composition was checked on a Beckman 6300 amino acid analyzer by total hydrolysis (6N HCl at 110 °C for 18–20 h) and by mass spectrometry. The final peptide purity was greater than 99%.

NMR relaxation experiments

^{13}C NMR measurements were performed on a Bruker AMX-500 spectrometer at a ^{13}C frequency of 125 MHz. The temperature, which was varied from 278 to 343 K, was calibrated by measuring 1,2-dihydroxyethane ^1H chemical shifts. Spin–lattice relaxation was monitored by the inversion-recovery method with and without broadband proton decoupling. The number of acquisitions was varied from 32 to 1024 (for ^{13}C proton-coupled relaxation) in order to maintain a signal-to-noise ratio greater than 6. At least 10 partially relaxed spectra were acquired for each relaxation experiment. To reduce errors from radiofrequency field inhomogeneities, the composite 180° pulse (90°_x-180°_y-90°_x) was used.

Auto- and cross-correlation times τ_{CH} and τ_{HCH} were calculated from initial relaxation rate curves by using Eqs. 1a and 1b. To minimize the error in determining these rates, a least-squares method with weighted functions, e.g., $A(t)=\exp(-2W_W t)$, was used. W_W was calculated by minimizing the function $\Sigma_i(I_0 - I_i - A\exp(-W_W t_i))^2$, where I_0 and I_i are equilibrium and transient values, respectively, of resonance intensities. To calculate the relaxation rate, W, the function

$$S = \sum_i \exp(-2W_W t_i)\,(I_0 - I_i - A\exp(-W t_i))^2 \qquad (17)$$

was minimized. This method reduces errors arising from inaccuracies normally present at the tail of relaxation curves plotted on the semilogarithmic scale. Statistical errors in determining spin–lattice relaxation rates were less than about 5%.

Computer modeling

Computer modeling was used to provide a more physically meaningful picture of the influence of overall tumbling and internal rotations on motional correlation times. Molecular dynamics calculations were performed for peptides in water by using standard AMBER potential energy parameters in the DISCOVER program (Version 2.9; Biosym Technologies, Inc.). All calculations were done by using four R4400 CPUs operating on a Silicon Graphics Challenge-L computer. Periodic boundary conditions were applied to a $20\times20\times20$ Å cell with a cutoff distance of 10 Å. Each simulation ran 5×10^5 steps with a time step of 1 fs. Molecular coordination files were recorded every 500 steps following stabilization of the total energy (about 2.5×10^4 steps). Input files for molecular dynamics runs were the result of conjugate gradient minimizations of each peptide/water system.

To check the role of rotational fluctuations, stochastic dynamics modeling (Daragan and Mayo, 1994) was done. Previous MD minimization provided peptide coordinates. To generate different peptide conformations, φ, ψ and χ angles were rotated and resulting structures were taken as 'equilibrium' conformations. Internal rotational fluctuations were viewed as jumps between two states $\gamma_o-\gamma$ and $\gamma_o+\gamma$, where γ_o is the equilibrium value of one of the φ, ψ and χ peptide backbone and side-chain angles, and γ is the amplitude of rotational fluctuations. For GK and KG, $2^6=64$ states were considered for φ, ψ, χ_1, χ_2, χ_3 and χ_4 rotations. Transition probabilities between i and j states (i,j = 1,2,...,64), W_{ij}, were calculated under the assumption that:

$$W_{ij} \propto \left[\sum_k (\mathbf{R}_i^k - \mathbf{R}_j^k)^2\right]^{-0.5} \qquad (18)$$

where $\mathbf{R}_i^k$ is the coordinate vector of the *k*th peptide atom in the laboratory frame for the *i*th state. Equation 18 approximates peptide/water interactions during rotational fluctuations: the smaller the changes in peptide orientation during internal rotations, the fewer the perturbations to the water structure. By using this approach, correlations of internal rotations are also accounted for: to reduce distortions in peptide geometry, simultaneous rotations about different bonds were allowed. Such transitions were found to be preferable when peptide geometry distortions were minimal. Strong correlations (large values of W_{ij}) were found when $\Delta\psi_1\Delta\varphi_2<0$, $\Delta\chi_1\Delta\chi_3<0$, $\Delta\chi_2\Delta\chi_4<0$, $\Delta\chi_2\Delta\chi_3>0$ or $\Delta\chi_3\Delta\chi_4>0$. Backbone rotational ($\Delta\psi_i,\Delta\varphi_{i+1}$) correlations are well known from molecular dynamics simulations of proteins and short peptides (McCammon et al., 1977; García, 1992).

Using a stochastic dynamics approach, auto- and cross-correlation functions were calculated by using Eqs.

3 and 4, and the corresponding correlation times were estimated via integration of these functions. For each time point in a correlation function, at least 10^5 values were calculated with successive averaging.

Results

^{13}C NMR relaxation data

The pH dependence of auto- and cross-correlation times for GK, KG and GKG C-H bond rotations is shown in Figs. 2A–C. Regardless of position in the sequence, glycine $C_\alpha H$ auto-correlation times are always less than those for lysine $C_\alpha H$ rotations. This is consistent with the expected greater rotational freedom for glycine relative to that for the bulkier lysine residue. In KG, τ_C of the C-terminal glycine is largest at pH 2. The same observation has been made for triglycine (Daragan and Mayo, 1993b). The COOH group has a greater potential for hydrogen bond formation with solvent water molecules, thereby reducing motional amplitudes. The N-terminal glycine $C_\alpha H$ in GK gives the smallest τ_C value at pH 10, where titration of the protonated amine reduces the number of potential NH/water hydrogen bonds, thereby increasing rotational mobility (Daragan and Mayo, 1993). In GKG at pH 6, correlation times of C-terminal

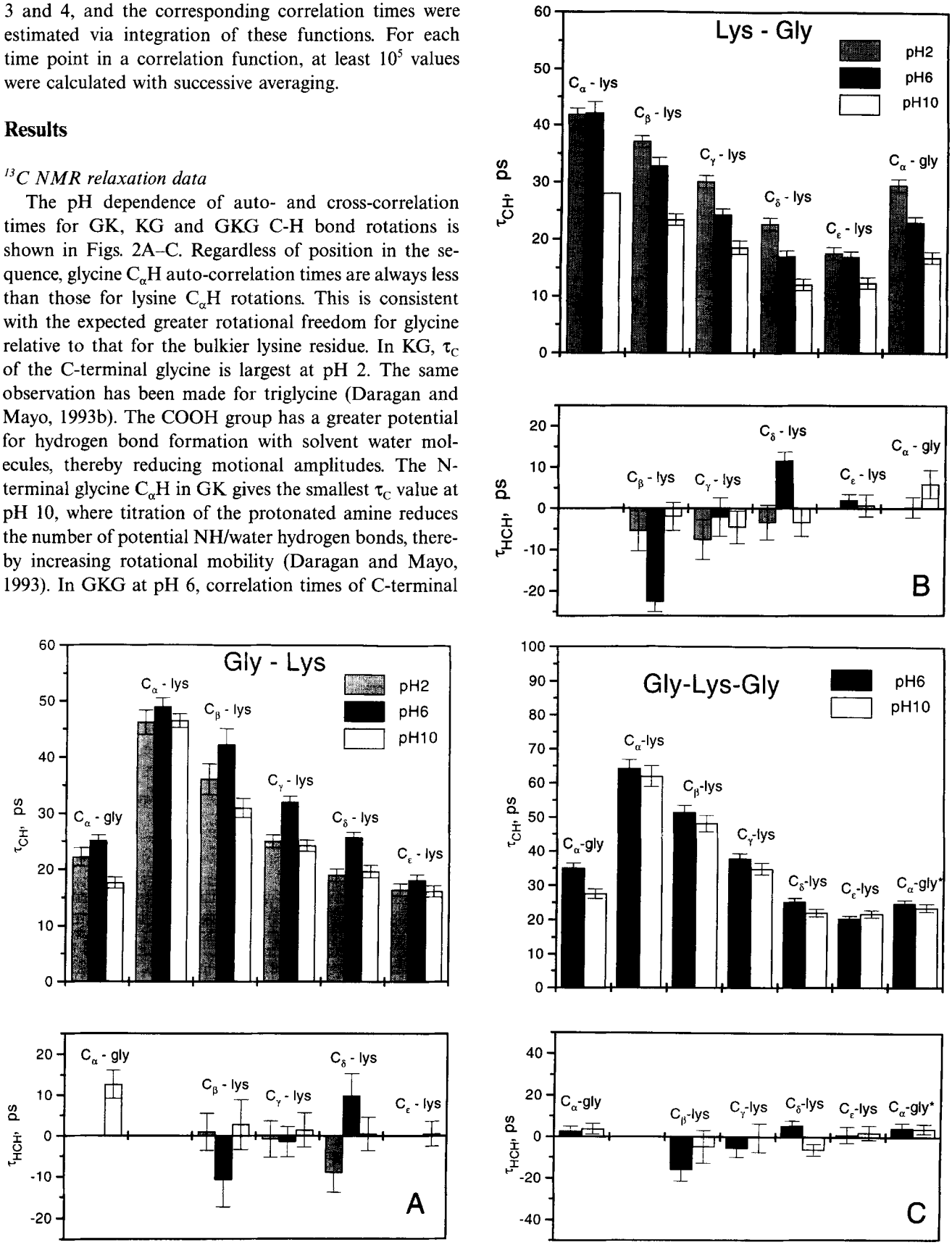

Fig. 2. Auto- and cross-correlation times of rotational motions of different CH bonds for (A) GK, (B) KG and (C) GKG. Data are given for 298 K and at pH values of 2, 6 and 10 as indicated in the figure. The peptide concentration in water was 30 mg/ml. For GKG, values for the C-terminal glycine are indicated with an asterisk.

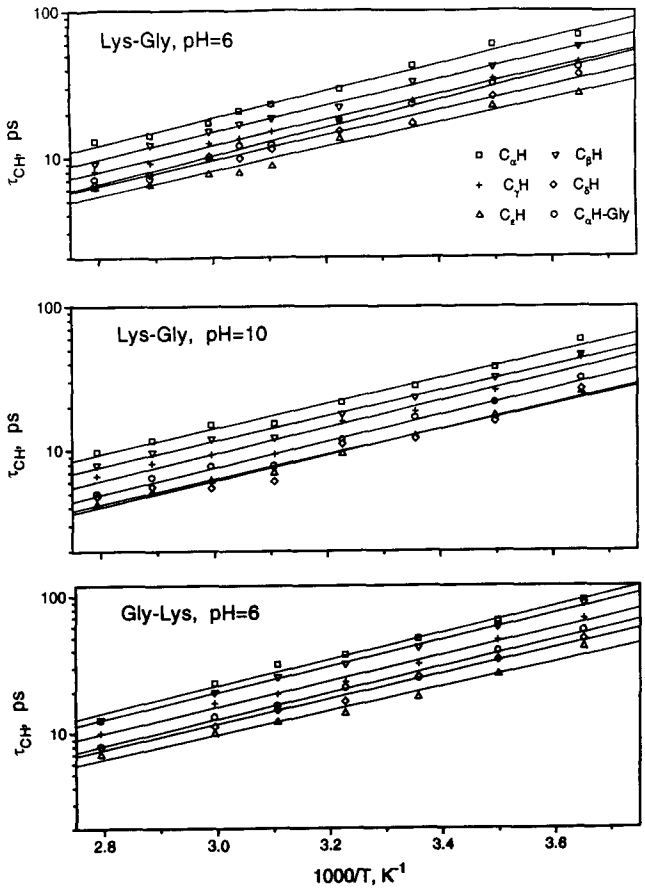

Fig. 3. The temperature dependence of auto-correlation times for different CH-bond rotations in GK and KG. The peptide concentration in water was 30 mg/ml.

glycine rotations are unexpectedly shorter than those for N-terminal glycine rotations; they become approximately equal at pH 10. Qualitatively, the pH dependence of auto- and cross-correlation times for N- and C-terminal glycines is similar for GGG (Daragan and Mayo, 1993) and for GK, KG and GKG.

In all peptides, lysine side-chain motions increase (τ_{CH} decreases) on going from C_β to C_ε. Lysine side chains in GK and KG, however, display somewhat different pH dependencies. In GK, lysine side-chain τ_{CH} values are maximal at pH 6 (fully charged state), whereas those in KG decrease with increasing pH. In GKG, the τ_C pH dependence is not as pronounced. This effect is attenuated for lysine side-chain dynamics in GKG.

There are two possible explanations for observed lysine side-chain rotational correlation time differences among GKG, KG and GK: (i) intermolecular associations; and (ii) intramolecular interactions. Either possibility is probably electrostatically modulated. Since the effect is highly reduced for GKG relative to KG and GK, intramolecular interactions probably do contribute to the observed differences. To check for intermolecular associations, however, KG auto-correlation times were measured over a peptide concentration range of 5 to 100 mg/ml (data not shown). Only $C_\alpha H$ auto-correlation times are, within error, slightly affected. On decreasing the concentration 20-fold, τ_{CH} is decreased at most by about 15%. Since no significant concentration dependence was observed for lysine side-chain τ_{CH} values, one may conclude that associations which do occur do so via interactions between N- and C-terminal charged groups. Conclusions drawn about lysine side-chain dynamics, therefore, are apparently independent of this association process and primarily reflect intramolecular interactions.

Since the τ_{CH} temperature dependence for GK and KG appears linear (Fig. 3), the Arrhenius equation was used in least-squares fits of these data to yield activation energies, E_{CH}, given in Table 1. E_{CH} values are close to those previously measured for triglycine (Daragan and Mayo, 1993b). Although absolute values of correlation times are relatively sensitive to pH, E_{CH} does not vary significantly with pH. Based on the observation that E_{CH} shows minimal pH dependencies and is essentially invariant for different peptides, one may conclude that peptide–water interactions primarily influence overall tumbling and internal motions of these short peptides.

Cross-correlation times for GK, KG and GKG are given in Figs. 2A–C. At 125 MHz and pH 2 or 6, glycine C_α and lysine C_ε resonances overlap for GK and GKG. Therefore, some cross-correlation times were measured at a ^{13}C frequency of 90 MHz. Irrespective of experimental errors indicated for τ_{HCH} values, one can conclude that cross-correlation times for all peptides show the same qualitative trends. Most significant is the observation that in the zwitterionic state, $C_\beta H_2$ and $C_\delta H_2$ lysine side-chain groups demonstrate large negative and positive signs, respectively, in their rotational cross-correlation terms. These τ_{HCH} values change sign and are attenuated when the ionization state is changed at low or high pH. For all other carbons, cross-correlation times tend to remain closer to zero, with the exception of the GK glycine $C_\alpha H_2$

TABLE 1
ACTIVATION ENERGIES OF AUTO-CORRELATION TIMES FOR GK AND KG PEPTIDES[a]

Peptide	E_{Gly}	E_α	E_β	E_γ	E_δ	E_ε
KG (pH = 6)	4.4 (0.2)	4.2 (0.2)	4.1 (0.1)	4.0 (0.1)	3.9 (0.2)	3.8 (0.2)
KG (pH = 10)	4.2 (0.2)	4.0 (0.2)	4.0 (0.2)	4.2 (0.3)	3.9 (0.4)	4.1 (0.2)
GK (pH = 6)	4.4 (0.2)	4.5 (0.2)	4.5 (0.1)	4.4 (0.2)	4.3 (0.2)	4.1 (0.3)

[a] Activation energies in kcal/mol. Experimental errors are given in parentheses.

TABLE 2
BACKBONE AND SIDE-CHAIN DIHEDRAL ANGLES FOR DIPEPTIDES GK AND KG[a]

Peptide	$D_\perp/D_\parallel$	ψ_1^0	φ_2^0	χ_1^0	χ_2^0	χ_3^0	χ_4^0
GK[b] (tttt)	0.23	146	−142	−173	177	179	179
GK (tg^-g^-t)	0.31	−85	−86	−157	−61	−67	105
GK (tg^-tg^-)	0.30	−77	−71	−179	−93	140	−83
GK (tg^+tg^+)	0.28	−78	−72	169	57	−148	68
GK[c] (tttt)	0.40	−84	−145	−167	179	−176	178
KG[b] (tttt)	0.43	−136	133	−170	−179	178	−178
KG (tg^-tg^-)	0.60	−84	122	−179	−100	−174	−79
KG (tg^+tg^+)	0.62	92	125	177	66	174	75
KG ($tttg^-$)	0.58	−88	144	−167	−154	170	−75
KG[c] (tttt)	0.35	124	−172	−169	−179	−180	−178

[a] All dihedral angles are in degrees and were obtained by energy minimization with and without electrostatic interactions using standard AMBER potentials in the DISCOVER program. The χ_1 angles are for N-C_α-C_β-C_γ moieties of lysine residues. Given in parentheses are the minimization starting conformations of the lysine side chain. Starting angles of ψ_1 and φ_2 peptide backbone rotations were equal to 180°. The ratios of diffusion coefficients calculated from the modified Kirkwood–Steel–Huntress theory are also presented.
[b] The results of calculations without electrostatic interactions.
[c] The results of calculations for pH = 10 (all other data are for pH = 6).

(pH = 10). Since cross-correlation times at 90 MHz for GK (pH 6 and 100 mg/ml) are $\tau_{HCH}(Gly) = 3.3 \pm 1$ ps, $\tau_{HCH}(C_\beta) = -28 \pm 5$ ps, $\tau_{HCH}(C_\gamma) = -9.8 \pm 3$ ps, $\tau_{HCH}(C_\delta) = 4.5 \pm 2$ ps, and $\tau_{HCH}(C_\varepsilon) = -0.4 \pm 1$ ps, it is apparent that even at high concentration, cross-correlation times follow the same trend. In any event, electrostatic interactions significantly affect lysine side-chain motional dynamics in GK, KG and GKG peptides.

Computer simulations

φ, ψ, χ_1, χ_2, χ_3 and χ_4 bond rotational energy profiles were calculated by using the Biosym suite of programs with standard AMBER potentials. Although it is recognized that solvent–peptide interactions will have some effect on rotational amplitudes and energetics, calculations were performed in vacuo for simplicity. GK and KG starting structures (see Table 2) were chosen from energy-minimized conformations with the lowest minima. Screening from polar water molecules attenuates electrostatic interactions and therefore influences the amplitudes and positions of rotational energy barriers. Calculation of motional parameters, however, does not depend significantly on small conformational changes in the peptides, and only conformations which are presented in Table 2 have been used.

Molecular dynamics calculations for GK in water will be presented to illustrate the stability of 'equilibrium' conformations and the role of conformational jumps on peptide dynamics. The time dependencies of GK φ, ψ, χ_1, χ_2, χ_3 and χ_4 dihedral angles at pH = 6 and pH = 10 are

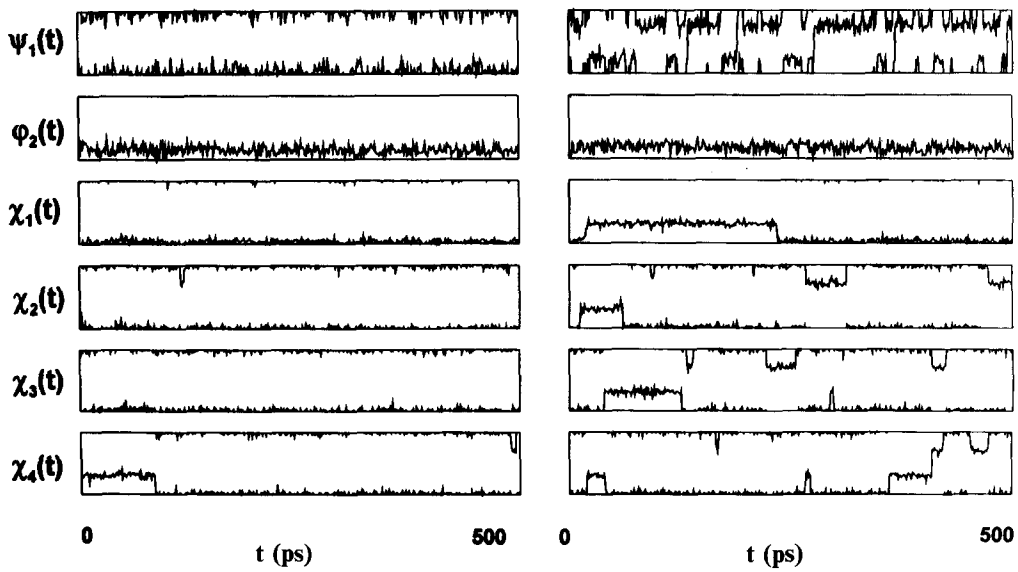

Fig. 4. The time dependence of various dihedral angle fluctuations in GK, taken from a molecular dynamics simulation in water. A 500 ps run with a sampling period of 1 ps is shown. The y-axes on each graph vary from −180° to 180°. Electrostatic potentials have been varied to approximate pH values of 6 (left) and 10 (right). The simulation temperature was 350 K. Standard AMBER potentials were used in all calculations.

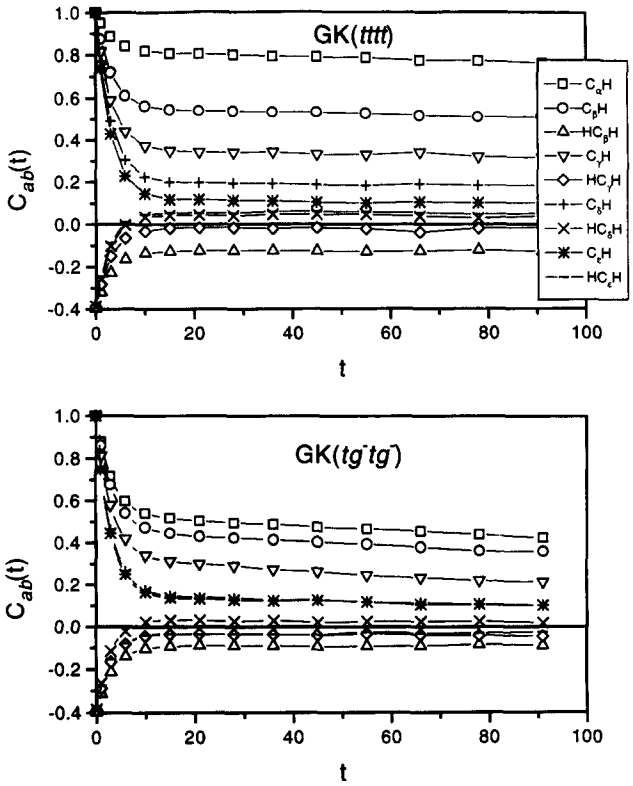

Fig. 5. Internal auto- and cross-correlation functions, $C^i_{ab}(t)$, for different CH-bond rotations in GK, calculated by using stochastic dynamics modeling. Two different equilibrium peptide conformations were used (see Table 2). Time units are given in terms of 3τ, where τ is the average correlation time for rotational fluctuations.

given in Fig. 4. Shortly after initiation of the calculation from the equilibrium structure, the lysine side-chain conformation became all-trans for whichever starting conformation was chosen at pH = 6. The all-trans conformation was relatively stable during the entire 500 ps run. However, rotational fluctuations and a few conformational jumps were observed. Backbone bond rotational fluctuation amplitudes were significantly larger than those for the lysine side chain. It appears that rotational fluctuations within potential energy minima are important and may dominate lysine side-chain internal motions in GK, KG and GKG. This view is consistent with activation energy barriers calculated from the temperature dependence of auto-correlation times. These barriers are relatively large (about 5 kcal/mol) with respect to the kinetic energy of a single bond rotation. Moreover, the apparent infrequency of conformational jumps suggests that rotational fluctuations dominate lysine side-chain internal motions and therefore contribute most to observed rotational correlation times and measured values of E_{CH}. Large-amplitude rotational fluctuations within a peptide (or protein) disturb surrounding water molecules. For GK, KG and GKG, this is apparent since E_{CH} values are approximately equal to the activation energy barrier for the viscosity of water (4.6 kcal/mol) (Tyrrell, 1961). At pH 10, the lysine side chain becomes more mobile (Fig. 4). These calculations illustrate the importance of electrostatic interactions in stabilizing peptide conformation.

Stochastic dynamics calculations (Daragan and Mayo, 1994) provide a simple approach to obtain various model parameters from ^{13}C NMR relaxation data. Calculated correlation functions are exemplified in Fig. 5. These calculations were performed on GK from an 'equilibrium' (tttt) and (tg^+tg^+) lysine side-chain conformation (Table 2). Rotational fluctuation amplitudes are the following: $\Delta\psi_1 = 100°$, $\Delta\varphi_2 = 70°$, $\Delta\chi_1 = 30°$, $\Delta\chi_2 = 30°$, $\Delta\chi_3 = 30°$, and $\Delta\chi_4 = 30°$. In Fig. 5, only internal correlation functions $C^{int}_{ab}(t)$ (see Eq. 4) are shown. Various decay rates for auto- and cross-correlation functions have been determined with transition probabilities between various rotomer 'states', as described previously (Daragan and Mayo, 1993b). Using Eq. 5 and data presented above, one can approximate auto- and cross-correlation functions by using the 'model-free' Eq. 19:

$$C^{int}_{ab}(t) = (0.5(3\cos^2\theta_{ab} - 1) - S^2_{ab})\exp(-t/\tau_i) + S^2_{ab} \quad (19)$$

For the auto-correlation function (a = b), Eq. 19 becomes the well-known Lipari–Szabo equation:

$$C^{int}_{aa}(t) = (1 - S^2_{aa})\exp(-t/t_i) + S^2_{aa} \quad (20)$$

where S^2_{aa} are order parameters (Lipari and Szabo, 1982; Kay and Torchia, 1991). Comparison of calculated correlation functions and NMR relaxation data will be discussed below.

Analysis and Discussion

Simple analysis of glycine motions

In all peptides, glycine residues are relatively mobile, as can be seen from molecular dynamics trajectories (Fig. 4). Coupling coefficients, K, are probably close to one due to large differences in the moments of inertia of glycine and the remainder of the peptide. Overall peptide tumbling, therefore, is essentially independent of internal rotations about the ψ_1 bond in GK and about the φ_2 bond in KG. Under this assumption, we can write general equations for auto- and cross-correlation times (Daragan and Mayo, 1993b) for tetrahedral geometry of the methylene group:

$$\tau_{CH} = S^2_{CH}\tau_0 + (1 - S^2_{CH})\,\tau_0\tau_i/(\tau_0 + \tau_i) \quad (21a)$$

$$\tau_{HCH} = S^2_{HCH}\tau_0 + (-1/3 - S^2_{HCH})\,\tau_0\tau_i/(\tau_0 + \tau_i) \quad (21b)$$

where τ_i is the correlation time of internal rotation. The overall tumbling correlation times, τ_0, in Eqs. 21a and 21b may be interpreted as the correlation time for reorientation of the $C1_\alpha$-C1 bond in GK and GKG (for the N-terminus), the N2-$C2_\alpha$ bond in KG and the N3-$C3_\alpha$ bond

TABLE 3
ROTATIONAL AUTO- AND CROSS-CORRELATION TIMES AND PARAMETERS OF RESTRICTED MOTIONS OF GLYCINE RESIDUES IN GK, KG AND GKG AT DIFFERENT pHs AT 298 K[a]

Peptide	pH	τ_{CH}	τ_{HCH}	τ_0	2γ	S^2_{CH}
Gly-Lys	2	22	–	–	–	–
Gly-Lys	6	25	–	–	–	–
Gly-Lys	10	18	6	90	180	0.20
Gly-Lys[b]	6	29	3.3	110	160	0.27
Lys-Gly	2	30	–	–	–	–
Lys-Gly	6	23	0.3	75	150	0.34
Lys-Gly	10	17	6	90	180	0.20
*Gly-Lys-Gly	6	35	2.5	120	150	0.30
Gly-Lys-*Gly	6	25	4.3	100	160	0.24
*Gly-Lys-Gly	10	28	3.7	105	160	0.26
Gly-Lys-*Gly	10	25	2.6	91	150	0.28

[a] All correlation times are in ps. The angles γ (°) are determined from a model of rotational restricted diffusion. Errors in determinations of τ_{CH} are 1 ps; errors in determinations of τ_{HCH} are 2–3 ps.
[b] Results at a peptide concentration of 100 mg/ml and a ^{13}C NMR frequency of 90 MHz. Some data are missing because of overlap of NMR multiplet lines. Errors in determination of 2γ are about 20°; errors in determination of τ_0 are 10–15 ps.

in GKG. For many models of one-axis rotations, S^2_{HCH} can be written as (Daragan and Mayo, 1993b)

$$S^2_{HCH} = (1 - 3S^2_{CH})/6 \quad (22)$$

The order parameters S^2_{CH} and S^2_{HCH} depend on internal rotational restrictions. For example, if we consider the model of two-state rotational jumps between $\gamma_0 - \gamma$ and $\gamma_0 + \gamma$ (Tsutsumi, 1979; Daragan and Mayo, 1993b), then

$$S^2_{CH} = 1 - (8/27)\sin^2\gamma(1 + 8\cos^2\gamma) \quad (23)$$

For the model of restricted rotational diffusion with specific boundary limits (London and Avitable, 1978; Wittebort and Szabo, 1978; Daragan and Mayo, 1993b), S^2_{CH} can be approximated by:

$$S^2_{CH} = 1 - (8/9)(1 - \sin^2\gamma/(3\gamma^2)(1 + 2\cos^2\gamma)) \quad (24)$$

For the model of rotational fluctuations within a potential well(s), the internal correlation time, τ_i, is much less than the correlation time of overall tumbling, τ_0. In this case, the second terms in Eqs. 21a and 21b vanish, and one can estimate τ_0 and S^2_{CH} from the experimental values of τ_{CH} and τ_{HCH}. Rotational restriction limits, 2γ, for the model of restricted rotational diffusion also have been determined. The model of rotational jumps was not used here because there are multiple solutions of Eq. 23 for large values of γ. For simplicity, conformational jumps over barriers and rotational fluctuations within potential wells will not be differentiated, and the values of γ will be used to describe the average values of internal rotational restrictions. Values of 2γ and S^2_{CH} are given in Table 3.

For GK and GKG at high pH, the N-terminal glycine is deprotonated, making it less bulky and less able to form hydrogen bonds with solvent water molecules. This, in turn, leads to an increase in GK glycine and GKG N-terminal glycine mobilities, as reflected in the values of S^2_{CH} and τ_0. In KG, a decrease in glycine rotational mobility at low pH can be explained by following the same reasoning, while an increase in glycine rotational mobility at high pH is apparently the result of reduced intramolecular electrostatic interactions. Large values of 2γ, obtained from the model of restricted rotational diffusion, indicate that large-amplitude conformational jumps significantly influence terminal glycine internal rotations. These values are in good agreement with the molecular dynamics simulations shown in Fig. 4. In the zwitterionic state, mobility of G3 in GKG is greater than it is for G1 in triglycine (Daragan and Mayo, 1993b). As shown in Fig. 6, this is the result of different energy profiles for ψ_1 and φ_3 rotations, which are quite similar to those in triglycine.

Model of multiple restricted uncoupled rotations

Based on the approach described by Wittebort and Szabo (1978), a model of multiple restricted uncoupled rotations can be defined by using a molecular frame with respect to the peptide and by estimating the components of the rotational diffusion tensor and its orientation within this frame. To evaluate these diffusion tensor components, calculations using the modified Kirkwood–Steel–Huntress theory (Eq. 10) were performed for KG and GK. To estimate the possible influence of water–peptide interactions, calculations were also performed for peptide/water complexes with different numbers of water molecules, under the assumption that the orientation of the rotational diffusion tensor coincides with that of the tensor of the moment of inertia. Calculations on GK with an all-trans lysine side-chain conformation yield the ratio $D_\perp/D_\parallel = 0.23$ [$D_\parallel = D_{ZZ}$, $D_\perp = (D_{XX} + D_{YY})/2$]. The value of D_{XX}/D_{YY}, which characterizes the deviation from a sym-

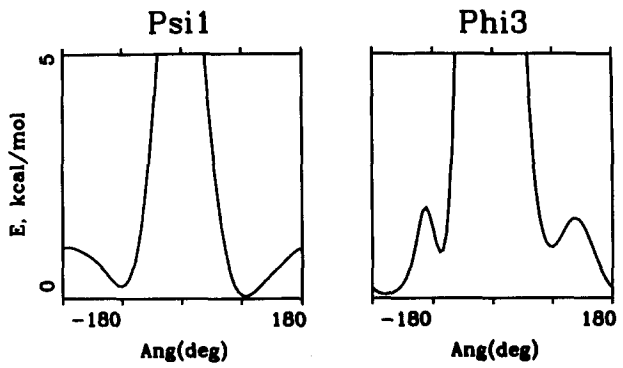

Fig. 6. Energy profiles for ψ_1 and φ_3 rotations in GKG, calculated in vacuo by the DISCOVER program.

metric top-type rotation, is equal to 1.23. The ratio 0.23 is close to the anisotropy value estimated from the tensor of the moment of inertia: $2I_{ZZ}/(I_{XX}+I_{YY})=0.24$, whereas the ratio of D_{XX}/D_{YY} is greater than $I_{YY}/I_{XX}=0.86$. I_{XX}, I_{YY} and I_{ZZ} are components of the moment of inertia tensor. Adding water to the carboxylate and amine groups modifies the rotational anisotropy slightly: $D_\perp/D_\parallel=0.24$ and $D_{XX}/D_{YY}=1.29$. These ratios were calculated for a peptide complexed with four and three water molecules to the carboxylate and amine groups, respectively. Since D_{XX}/D_{YY} is close to 1, one can use the symmetric top approximation to describe overall peptide tumbling. $D_\perp/D_\parallel$ values for other trans/gauche conformations of GK and KG are given in Table 2.

Intermolecular interactions change the orientation of the rotational diffusion tensor with respect to the orientation of the moment of inertia tensor. To describe such reorientations, the molecular coordinate system centered on the C_α atom of lysine has been chosen. The y- and z-axes lie in the plane formed by N, C_α and C atoms, with the z-axis bisecting the N-C_α-C angle and directed toward the lysine side chain. The x-axis is perpendicular to this plane. For symmetric top rotational diffusion, only four parameters need to be determined: the polar angles of the z_D-axis of the diffusive frame with respect to the molecular frame, θ_D and ϕ_D and the components of the diffusion tensor: $D_\parallel=D_{ZZ}$ and $D_\perp=D_{XX}=D_{YY}$. Calculated correlation times depend on the conformation of the lysine side chain, i.e. dihedral angles χ_i^0 ($\alpha_{i-1,i}$ in Eq. 13), and on the conformation of the peptide backbone, i.e., φ^0 and ψ^0 dihedral angles. The superscript '0' was used here to denote equilibrium values of χ_i and φ,ψ angles. Two additional parameters need to be determined for each χ_i internal rotation: the internal rotational diffusion coefficient, D_i, and the angular restriction, $\Delta\chi_i$. The number of experimental parameters is not sufficient for an accurate fit. Therefore, to reduce the number of model parameters, some stable structures (Table 2) were determined from energy minimization calculations using the DISCOVER program. Electrostatic interactions were taken into account during these minimizations. Results are given in Table 5. There is no strong dependence of rotational anisotropy on the conformational state, but the difference between GK and KG peptides is substantial.

The fitting procedure given in Eq. 13 was used to determine the orientation of the rotational diffusion tensor (θ_D and ϕ_D angles), the correlation time of overall tumbling $\tau_\perp=1/6D_\perp$, the angular restrictions $\Delta\chi_i$ and the rotational diffusion coefficients for internal rotations D_i. $D_\perp/D_\parallel$ values were taken from Table 2 in order to reduce the number of fitting parameters. Calculations were performed for all peptide conformations listed in Table 2. To

TABLE 4
EXPERIMENTAL AND CALCULATED AUTO- AND CROSS-CORRELATION TIMES FOR DIFFERENT BONDS IN DIPEPTIDES GK AND KG[a]

Peptide	Gly $C_\alpha C$	Lys								
		$C_\alpha H$	$C_\beta H$	$HC_\beta H$	$C_\gamma H$	$HC_\gamma H$	$C_\delta H$	$HC_\delta H$	$C_\varepsilon H$	$HC_\varepsilon H$
GK (exp)	95	49	42	−11	32	0.1	26	9	18	−4
GK (tttt)	90	46	45	−11	31	−2	20	−1.1	25	−2
GK (tg^-g^-t)	83	48	49	−11	26	−5	22	−4	23	−2
GK (tg^-tg^-)	81	49	48	−11	25	−5	22	−2	22	−2
GK (tg^+tg^+)	82	47	47	−11	31	−5	22	2	22	−3
GK[b] (exp)	88	46	31	−9	24	3	20	−0.2	16	−1
GK[b] (tttt)	60	40	39	−9	24	2	22	3	19	4
KG (exp)	71	42	33	−23	24	−2	17	12	17	2
KG (tttt)	50	35	42	−22	22	−6	18	−3	17	−2
KG (tg^-tg^-)	50	39	43	−20	23	−3	18	−0.7	18	−2
KG (tg^+tg^+)	48	39	42	−20	22	−5	17	−1	17	−2
KG (ttg^-)	49	38	43	−19	23	−5	18	−2	17	−1
KG[b] (exp)	86	28	23	−2	19	−5	12	−4	12	0.7
KG[b] (tttt)	28	28	28	−2	17	−2	14	−0.3	14	−0.1

[a] Correlation times (ps) were calculated from a multiple restricted rotational diffusion model.
[b] Results of calculations for pH = 10. All other data are for pH = 6. Corresponding conformations were taken from Table 2.

TABLE 5
FITTING PARAMETERS DETERMINED FOR GK AND KG AT 298 K[a]

Peptide	$\tau_\perp$	$\Delta\theta$	θ_D	ϕ_D	$\Delta\chi_2$	D_2	$\Delta\chi_3$	D_3	$\Delta\chi_4$	D_4
GK (tttt)	92	36	133	277	69	16	59	43	85	>100
GK (tg^-g^-t)	84	59	13	306	141	14	120	>100	85	>100
GK (tg^-tg^-)	83	51	7	58	141	15	106	>100	85	>100
GK (tg^+tg^+)	84	32	169	247	45	>100	115	94	85	>100
GK[b] (tttt)	60	38	142	269	51	>100	44	>100	144	>100
KG (tttt)	55	89	61	301	116	14	116	>100	85	>100
KG (tg^-tg^-)	51	31	89	92	52	73	116	>100	85	>100
KG (tg^+tg^+)	50	28	93	95	150	13	110	>100	85	>100
KG (ttg^-)	50	35	89	268	52	>100	123	>100	85	>100
KG[b] (tttt)	48	47	33	31	141	22	40	>100	85	>100

[a] Data were obtained using a multiple restricted rotational diffusion model. All correlation times are in ps; angles are in degrees. Internal rotation diffusion coefficients are in $10^9\ s^{-1}$.
[b] Results of calculations for pH = 10. All other data are for pH = 6.

determine parameters for overall tumbling, the auto-correlation times for rotations of the glycine $C_\alpha C$ and lysine $C_\alpha H$, $C_\beta H$ bonds and the rotational cross-correlation times for lysine $HC_\beta H$ were all used under the assumption that the N-C_α-(C_β)-C lysine fragment is rigid. In GK, the $C_\alpha C$ glycine bond is approximately parallel to the N-C_α lysine bond, and in KG, the $C_\alpha C$ glycine bond is approximately parallel to the C_α-C lysine bond. For this reason, τ_0 (Table 3) can be used to estimate values for N-C_α and C_α-C bond tumbling correlation times.

Table 4 gives calculated auto- and cross-correlation times determined by using parameters listed in Table 5. Auto-correlation times are relatively well fit, with the exception of data for KG at pH 10. For the lysine side chain, this approach failed to determine the positive sign of the $HC_\delta H$ bond rotational cross-correlation time in both GK and KG at pH = 6. Although better fits can be obtained when the rotational diffusion anisotropy, $D_\perp/D_\parallel$, is less than 0.1, such values are unrealistic. The error in determining $\Delta\chi_i$ and τ_i is about 30%. The angles $\Delta\theta$ given in Table 5 characterize deviations of the z-axis of the moment of inertia and the rotation diffusion tensor. $\Delta\theta$ reflects the importance of intermolecular interactions for overall molecular rotation. For most conformations, deviations are around 30° and there is no significant difference between GK and KG. For some conformations, $\Delta\chi_2$ falls between 50° and 60° and is in good agreement with results for poly-L-lysine presented by Wittebort et al. (1980). In these shorter peptides, however, both $\Delta\chi_3$ and internal diffusion coefficients are substantially larger. The average fitting error for experimental correlation times is 6 ps for GK and 9 ps for KG. Optimal fitting was obtained for GK with a (tttt) lysine side-chain conformation (error = 4.5 ps) and for KG with a (tg^-tg^-) conformation (error = 8.5 ps). These conformations can be considered to be preferable or the most stable; they account best for the experimental data by using the model of multiple independent restricted internal diffusional rotations. Nevertheless, these fitting errors are approximately twice as large as average experimental errors, especially for cross-correlation terms where positive and negative signs cannot even be described. The sensitivity of cross-correlation functions to rotational anisotropy makes it imperative to develop a new approach to describe correlated internal rotations in lysine side chains (as well as in other amino acids with long alkyl groups).

Stochastic dynamics modeling

Computer modeling using the stochastic dynamics algorithm described above was done in an attempt to explain the different signs for cross-correlation times. Only lysine side-chain dynamics are considered in this section. The anisotropy of overall tumbling is most important for χ_1 rotations. For χ_2, χ_3 and χ_4 rotations, this anisotropy can be neglected. For the calculations, the following rotational amplitudes were considered: $\Delta\chi_1 =$

TABLE 6
ORDER PARAMETERS S^2_{ab} OF DIFFERENT BONDS FOR DIFFERENT CONFORMATIONS OF GK[a]

Conformation	$C_\alpha H$	$C_\beta H$	$HC_\beta H$	$C_\gamma H$	$HC_\gamma H$	$C_\delta H$	$HC_\delta H$	$C_\varepsilon H$	$HC_\varepsilon H$
(tttt)	0.79	0.54	−0.14	0.34	−0.02	0.19	0.04	0.1	0.05
(tg^-tg^-)	0.49	0.49	−0.14	0.32	−0.06	0.18	0.0	0.15	−0.09
(tg^+tg^+)	0.39	0.38	−0.09	0.26	−0.02	0.14	0.0	0.12	−0.07
(tg^-g^-t)	0.55	0.50	−0.14	0.35	−0.08	0.24	−0.08	0.13	−0.03

[a] Order parameters were calculated with a stochastic dynamics algorithm. All conformations are defined in Table 2.

TABLE 7
AUTO- AND CROSS-CORRELATION TIMES FOR GK AT 298 K[a]

pH	$C_\gamma H$	$HC_\gamma H$	$C_\delta H$	$HC_\delta H$	$C_\varepsilon H$	$HC_\varepsilon H$
2	26	–5	19	–4	13	–2
6	37	–2	21	4	14	2
10	26	–4	17	–1	13	–3

[a] All correlation times are in ps and were calculated with a stochastic dynamics algorithm.

$\Delta\chi_2 = \Delta\chi_3 = \Delta\chi_4 = 30°$, $\Delta\psi_1 = 100°$ and $\Delta\varphi_2 = 70°$. These values are consistent with molecular dynamics results and give the best fit to all experimental data, including cross-correlation times. Recoil coefficients calculated from the moments of inertia (Eq. 9) were used. It was assumed that internal rotation correlation times are much smaller than overall tumbling correlation times. In this case, Eq. 19 shows that $\tau_{ab} = S_{ab}\tau_0$. Order parameters S^2_{ab}, given in Table 6, were obtained from the plateau of calculated correlation functions $C^{int}_{ab}(t)$. Conformational states listed in Table 2 are considered to be equilibrium conformations, and calculations were performed for all states. The most interesting problem was to explain the sign of cross-correlation times for lysine $HC_\delta H$ rotations. Since this behavior is similar in these peptides, only results for GK will be presented. It has been assumed that experimentally determined correlation times represent an average over all conformational states. To simplify the calculations, only conformations presented in Table 2 will be considered. The correlation time can be approximated as:

$$\tau_{ab} = \tau_0 \sum_i c_i S^i_{ab} \qquad (25)$$

where c_i is the fraction of the ith conformation, and S^i_{ab} is the corresponding conformational order parameter. The overall correlation time, τ_0, was obtained by minimizing the function:

$$s = \sum (\tau_{ab}(exp) - \tau_{ab})^2 \qquad (26)$$

where summation was performed over all experimentally determined correlation times $\tau_{ab}(exp)$. Table 7 gives the auto- and cross-correlation times calculated from S_{ab} and τ_0. The value of $\tau_0 = 95 \pm 10$ ps best describes the experimental data and is in good agreement with the value of $\tau_\perp$ derived from the model of multiple restricted diffusion rotations. This approach (Table 7) gives the correct sign for cross-correlation times and is better able to describe the experimental data than is the model of multiple restricted diffusion rotations. By using Eqs. 25 and 26, simple minimization was performed to estimate the conformational fraction. Consistent with molecular dynamics simulations, the (tttt) conformation is preferred at pH = 6. At low and high pH values, the fraction of the all-trans lysine side-chain conformation decreases to about 40%, while (tg^+tg^+) and (tg^-g^-t) conformational populations increase accordingly. Results at pH = 10 are consistent with molecular dynamics data (Fig. 4) which indicate more frequent rotational jumps in the lysine side chain. Although these results should be considered qualitative, one can conclude that the model of correlated fluctuations can describe both auto- and cross-correlation times better than the model of independent internal rotations, even when anisotropic overall tumbling is taken into account.

Conclusions

The results presented here serve to illustrate the sensitivity of cross-correlation spectral densities to peptide backbone and side-chain internal rotations. ^{13}C NMR relaxation data for GK, KG and GKG could not be explained by any rotational model which treats various bond rotations independently, even taking into account anisotropic overall peptide tumbling. Changes in the sign and magnitude of lysine side-chain methylene cross-correlation times could be explained only by considering correlated internal rotations. This study also highlights the importance of electrostatic interactions in defining peptide dynamics. In the fully charged state, carboxy and amino groups stabilize backbone and lysine side-chain orientations, probably by forming water 'bridges' between charged groups. For GK, internal rotational mobility increases on reducing the charged state. In GKG and GGG (Daragan and Mayo, 1993), terminal glycines behave similarly, consistent with similar φ,ψ rotational energy profiles. A model parameterized for correlated internal rotations and coupled overall tumbling/internal rotations had relative success in describing lysine side-chain dynamics. More simplified approaches, however, need to be developed to more easily obtain internal bond rotation parameters from NMR relaxation data.

Acknowledgements

This work was supported by a National Research Council/National Science Foundation International Project Development grant and by an NSF research grant (MCB-9420203) to K.H.M. We are grateful to Eric Eccleston and Denisha Walik of the Microchemical Facility for their patient cooperation during the synthesis of the peptides. NMR experiments were performed at the University of Minnesota High Field-NMR Laboratory.

References

Bain, A.D. and Lynden-Bell, R.M. (1975) *Mol. Phys.*, **30**, 325–356.

Daragan, V.A. and Mayo, K.H. (1992) *J. Am. Chem. Soc.*, **114**, 4326–4331.

Daragan, V.A. and Mayo, K.H. (1993a) *Chem. Phys. Lett.*, **206**, 393–400.

Daragan, V.A. and Mayo, K.H. (1993b) *Biochemistry*, **32**, 11488–11499.

Daragan, V.A. and Mayo, K.H. (1994) *J. Phys. Chem.*, **98**, 10949–10956.

Dellwo, M.J. and Wand, A.J. (1989) *J. Am. Chem. Soc.*, **111**, 4571–4578.

Dong, R.Y. and Richards, G.M. (1992) *Chem. Phys. Lett.*, **206**, 541–545.

Gaisin, N.K., Manyrov, I.R. and Enikeev, K.M. (1993) *Mol. Phys.*, **80**, 1047–1057.

García, A.E. (1992) *Phys. Rev. Lett.*, **68**, 2696–2699.

Gladkii, A.M., Daragan, V.A. and Edneral, I.V. (1987) *Sov. J. Chem. Phys.*, **4**, 825–830.

Grant, D.M., Mayne, Ch.L., Liu, F. and Xiang, T.-X. (1991) *Chem. Rev.*, **91**, 1591–1624.

Huntress, W.T. (1970) *Adv. Magn. Reson.*, **4**, 1–37.

Kay, L.E. and Torchia, D.A. (1991) *J. Magn. Reson.*, **95**, 536–547.

Knaus, D.C., Evans, G.T. and Grant, D.M. (1980) *Chem. Phys. Lett.*, **71**, 158–163.

Levine, Y.K., Birdsall, N.J.M., Lee, A.G., Metcalfe, J.C., Partington, P. and Roberts, G.C.K. (1974) *J. Chem. Phys.*, **60**, 2890–2899.

Lipari, G. and Szabo, A. (1982) *J. Am. Chem. Soc.*, **104**, 4546–4559.

London, R.E. and Avitable, J. (1978) *J. Am. Chem. Soc.*, **100**, 7159–7165.

McCammon, J.A., Gelin, B.R. and Karplus, M. (1977) *Nature*, **267**, 585–590.

Moro, G. (1987) *Chem. Phys.*, **118**, 167–180.

Nicholson, L.K., Kay, L.E., Baldisseri, D.M., Arango, J., Young, P.E., Bax, A. and Torchia, D.A. (1992) *Biochemistry*, **31**, 5253–5263.

Palmer III, A.G., Rance, M. and Wright, P.E. (1991) *J. Am. Chem. Soc.*, **113**, 4371–4380.

Steel, W.A. (1963) *J. Chem. Phys.*, **38**, 2404–2410.

Stewart, J.M. and Young, J.D. (1984) In *Solid Phase Peptide Synthesis*, 2nd ed. (Ed., Merrifield, J.) Pierce Chemical Co., Rockford, IL, p. 135.

Tsutsumi, A. (1979) *Mol. Phys.*, **37**, 111–127.

Tyrrell, H.J.V. (1961) *Diffusion and Heat Flow in Liquids*, Butterworths, London.

Vetrov, O.D., Daragan, V.A. and Edneral, I.V. (1984) *Sov. J. Chem. Phys.*, **1**, 2517–2527.

Weaver, A.J., Kemple, M.D. and Prendergast, F.G. (1989) *Biochemistry*, **28**, 8624–8639.

Weaver, A.J., Kemple, M.D., Brauner, J.W., Mendelson, R. and Prendergast, F.G. (1992) *Biochemistry*, **31**, 1301–1313.

Werbelow, L.G. and Grant, D.M. (1977) *Adv. Magn. Reson.*, **9**, 189–299.

Wittebort, R.J. and Szabo, A. (1978) *J. Chem. Phys.*, **69**, 1722–1736.

Wittebort, R.J., Szabo, A. and Gurd, F.R.N. (1980) *J. Am. Chem. Soc.*, **102**, 5723–5728.